

1 **Factors influencing the calorespirometric ratios of soil microbial metabolism**

2 N. Barros⁽¹⁾, L.D. Hansen⁽²⁾, V. Piñeiro⁽³⁾, C. Pérez-Cruzado⁽⁴⁾, M. Villanueva⁽¹⁾, J. Proupín⁽¹⁾, J.A
3 .Rodríguez-Añón⁽¹⁾:

4 ⁽¹⁾ Department of Applied of Physics. University of Santiago de Compostela. Spain

5 ⁽²⁾ Department of Chemistry and Biochemistry, Brigham Young University, Provo, UT 84602 USA

6 ⁽³⁾ Elemental Analysis service. RIAIDT. Lugo. University of Santiago de Compostela. Spain.

7 ⁽⁴⁾ Forest Inventory and Remote Sensing. Georg-August-University Göttingen. Germany.

8 Corresponding author: N. Barros e-mail: nieves.barros@usc.es

9 **Abstract**

10 Calorespirometric ratios of metabolism connect the metabolic activity with the nature of the substrate and
11 metabolic pathways being used by cells and microorganisms. Calorespirometric ratios have been
12 determined for many living systems including animals, plants, plant and animal cells, and many different
13 microorganisms, but application to soil is very recent. Calorespirometric ratios for soil are obtained by
14 simultaneous calorimetric measurements of heat and CO₂ rates from biodegradation of soil organic
15 matter. The purpose here is to gain a better understanding of the calorespirometric ratios in soil and to
16 assess the factors influencing the value, i.e. changes in the composition of the soil organic matter,
17 humidity, soil particle size, and soil management (e.g. conversion of pasture to forest). Results indicate
18 that calorespirometric ratios are sensitive to humidity, soil size fraction and the age of organic matter in
19 soils.

20 *Keywords:* Calorespirometric ratios, SOM, humidity, soil fractions, pasture, forest age..

21

22 **Introduction**

23 Direct measurements of CO₂ as an indicator of microbial degradation of soil organic matter (SOM) are
24 important because CO₂ data can be used to evaluate the impact of soil management on atmospheric CO₂.
25 Soil management practices impact the capacity of soil to sequester C, and thus exert a direct effect on
26 future climate change. Soil management needs to be developed on a sustainable basis that minimizes
27 global warming, which requires understanding the mechanisms that favor soil C sequestration.
28 Determination of the properties of SOM and relating those properties with biodegradability is the basis
29 for the concept of SOM stabilization (Field et al. 2007; Connat et al. 2011). This concept has led to many
30 studies about SOM by a wide range of different methodologies providing chemical, physical and
31 biological SOM properties. Among those methods, thermal analysis involves easy and fast procedures
32 that yield data on the physical properties of SOM (Plante et al. 2009; Barros et al. 2007) while
33 calorimetry provides a means for direct measurements of the rates of microbial processes by
34 combined measurements of the rates of heat and CO₂ production by microbial metabolism (Matheson et
35 al. 2004; Hansen et al. 2004; Battley, 2013).

36 Soil calorimetry has the potential to provide a more complete description of microbial processes
37 related to the carbon cycle than do measurements of microbial CO₂ production alone (Herrmann et al.
38 2014). For example, combining measurements of the heat and CO₂ rates of soil microbial metabolism
39 allows application of thermodynamic models of the efficiency of soil microbial processes for retaining C
40 (Barros and Feijoo, 2003; Harris et al. 2012).. The mass-specific heat and CO₂ rates are quantitatively
41 informative about the rates of bioprocesses in soil, but either alone provides little information on the
42 nature of the organic substrate being degraded or on the efficiency of degradation processes. To close this
43 gap, concepts based on the calorimetric ratio (R_q/R_{CO_2}) in soils have been introduced, but not fully
44 developed. Previous applications to living systems showed R_q/R_{CO_2} ratios inform about the nature of the
45 substrate being degraded by microorganisms and about the efficiency of the metabolism, resulting an
46 attractive option if applied to soil research, that would enrich the knowledge about soil biochemistry.
47 Interpretation of calorimetric ratios for soils with a stoichiometric model of metabolism is an
48 attractive option to study microbial systems degrading complex substrates (Wadsö et al. 2004) Recent
49 papers (Barros et al. 2010; Barros et al. 2011) showed that calorimetric ratios measured on different
50 soils differed greatly, but the factors affecting the value of this ratio for soil microbial metabolism could
51 not be clearly identified.

52 A clear understanding of Thornton's rule, i.e., the enthalpy change for oxidation of any organic material
53 by O₂ is approximately constant when expressed per mole of O₂ (Hansen et al. 2004), is required for
54 interpreting calorespirometric ratios. The value of this approximate constant, the oxycaloric ratio (ΔH_{O_2}),
55 varies from -430 to -470 kJ per mole O₂, depending on conditions and the class of compound being
56 oxidized. The average value, -455 kJ/mol O₂ thus has a range of ± 15 kJ/mol O₂ or $\pm 3.3\%$.

57 In steady-state aerobic systems with no net growth of microorganisms, the calorespirometric ratio is given
58 by:

$$59 \quad R_q/R_{CO_2} = -\Delta H_{O_2}[1 - (\gamma_s/4)] = (455 \pm 15)[1 - (\gamma_s/4)] \quad (1)$$

60 where $-\Delta H_{O_2}$ is Thornton's constant (455 kJ/mol O₂) and γ_s is the oxidation state of the substrate carbon.
61 Under these conditions, R_q/R_{CO_2} depends solely on the oxidation state of the substrate. However, note that
62 γ_s is the oxidation state of the substrate carbon being oxidized to CO₂, not the average oxidation state of
63 the SOM. Therefore, if the ratio is measured at steady state with no microbial growth, comparison of
64 R_q/R_{CO_2} values obtained experimentally to those expected from the main substrates constituting the SOM
65 provide information on the substrate being degraded by soil microorganisms. The presence of microbial
66 growth is typically apparent from an exponentially increasing heat rate during a measurement, therefore
67 the steady state conditions can be easily monitored by calorimetry. Table 1 summarizes values of R_q/R_{CO_2}
68 for substances commonly found in soil organic matter for comparisons.

69 This work is focused on measuring R_q/R_{CO_2} of soil metabolism under steady-state conditions with no net
70 gain in microbial biomass, to determine how these ratios vary in soil under more controlled experimental
71 procedures than those reported previously (Barros et al. 2011). SOM physical properties are determined
72 by thermal analyses and ¹³C CPMAS to understand the effect of SOM properties on R_q/R_{CO_2} values and
73 R_q/R_{CO_2} values are determined under common soil treatments to see how conditions affect the ratio. The
74 goal is to improve knowledge about the factors influencing these ratios in soil for further application in
75 soil research on the metabolic paths involved in microbial metabolism responsible for SOM
76 biodegradation.

77 **2. Material and Methods**

78 2.1 Soil Samples

79 Soil samples used in this study represent an Alumi-humic regosol with inclusions of Alumi-humic
80 cambisols, Alumi-humic Umbrisols and District Cambisols (IUSS Working Group WRB 2006) collected
81 in Borreiros-Viveiro (43° 37' 51.94" N 7° 37' 22.63") and Castro del Rey (43° 12' 31" N 7° 24' 1" W)
82 Lugo, Spain. These samples were under different managements and vegetation (pasture, *Pinus radiata*
83 and *Eucalyptus nitens*).

84 The evolution of SOM properties and calorespirometric ratios with depth was determined with samples
85 of Aluminium regosol from Borreiros collected from 0-10 cm, 10-20 cm and 20-30 cm from the soil
86 surface. The sampling procedure was developed under standard statistical criteria to obtain representative
87 samples of the sampling area avoiding edge effects (Nuñez et al. 2006; Rodríguez-Añón et al. 2007). Two
88 plots were selected in the sampling area. In each of these, a 50x50 cm area was marked with 4 metal pegs
89 graduated from 0 to 50 cm. 4 soil sub-samples in each of the 50x 50 selected areas were extracted from 0-
90 10 cm, 10-20 cm and 20-30 cm from surface avoiding contamination among samples. In the laboratory, a
91 total of 8 subsamples were pooled by depth to one sample and sieved to 2mm. A portion of each soil
92 sample from different depths was dried at 105 °C in an oven during 24 h for elemental and thermal
93 analysis. Samples for calorespirometric measurements under different humidity percentages were air
94 dried at 21°C for 3 days. After this treatment these were stored in polyethylene bags at 4°C during one
95 month before the calorespirometric measurements to allow soils to stabilize after this treatment.

96 The influence of humidity on soil biodegradation and calorespirometric ratios was determined with soil
97 samples from different depths stored at 4°C. The water holding capacity (WHC) was determined prior to
98 storage using a glass tube fitted with a fritted glass disc in the bottom being immersed in water. The
99 humidity of the samples was measured by weight loss after drying at 105°C in an oven for about 24 h.
100 Biodegradation rates were measured after bringing the samples stored at 4°C to 13, 25, 38, 50, 62, 88 and
101 112% of WHC. For each calorespirometric measurement, 7 subsamples (10 g) of the soil from each depth
102 stored at 4°C for one month were first equilibrated at 25°C during 24 h inside polyethylene bags. After
103 this equilibration, subsamples from each depth were rewetted to the different humidity percentages and
104 incubated inside polyethylene bags at 25°C during 4 days before the calorespirometric measurements. The
105 incubation is done with a water container inside the polyethylene bags to maintain the vapor equilibrium
106 of the soils. The incubation period permits soil to stabilize after rewetting avoiding the measurement of
107 the initial flux of CO₂ and heat caused by the treatment. This behavior of the soil was previously tested by
108 calorimetry to check that after 4 days of incubation the heat rate was at a steady state.

109 The influence of mesh size and mechanical SOM fractionation on thermal properties and biodegradability
110 as measured by calorespirometry was determined with another sample of the Aluminiumric regosol
111 under *Pinus radiata* from 0-10 cm sieved at 2, 0.5 and 0.2 mm. Samples were sieved with an automatic
112 sieve shaker CISA RP 200N and the different fractions were characterized according to the grain size by
113 elemental and thermal analysis. Fractions for microbial metabolism measurements were air dried at 21°C
114 for 3 days and kept in polyethylene bags at 4°C.

115 The sensitivity of the calorespirometric ratios to different forest species and forest age was determined
116 with Alumi-humic Umbrisols and District Cambisols soil samples collected in the northwest of Spain in a
117 network of known chronosequences in this region (Castro del Rey) to. These soil samples were collected
118 in a pasture (used as a reference stand before afforestation) afforested with *Pinus radiata* and *Eucalyptus*
119 *nitens* (Pérez Cruzado et al. 2012; Pérez Cruzado et al. 2014). Afforested samples selected for this study
120 were those representing the rotation times of both tree species (30-40 yr for *Pinus radiata* and 18 years
121 for *Eucalyptus nitens* after afforestation). Three stands were selected for each of the tree species
122 representing different forest ages since afforestation: 10, 19 and 30 years for *Pinus radiata*, and 1, 5 and
123 18 years for *Eucalypt nitens*. Samples from a Pine forest with no previous history of afforestation was
124 used as forest reference. Soil sampling is explained in detail in a previous work involving the
125 chronosequence network (Pérez-Cruzado et al. 2014). A plot was established in each of the stands. In each
126 plot, six sampling points were established in a regular hexagonal frame. Six soil sub-samples were
127 collected with a steel corer at 0-10 cm depth and combined into one sample. Samples were sieved to 2
128 mm. This sampling procedure helps to make the calorespirometric ratios determined for each stand more
129 comparable with previous works reporting these values by similar sampling criteria. A portion of each of
130 the soil samples representing each stand was prepared for elemental and thermal analysis. The remainder
131 of each soil fresh sample was air dried at 21°C for 3 days to release the excess of water and then stored in
132 a polyethylene bag at 4°C for one month. Before calorespirometric measurements, 10 g of the soil from
133 each stand was equilibrated at 25°C during 24 h. After equilibration, samples were brought to 60% of
134 WHC and incubated inside polyethylene bags at 25°C during 4 days with a water container inside.

135 Elemental and Thermal Analysis

136 Carbon and nitrogen percentages were determined with a LECO Elemental analyzer.

137 Thermal properties of the samples were determined by thermogravimetry (TG) (TGA-DSC1 Mettler
138 Toledo) and differential scanning calorimetry (DSC) (Q200, TA Instruments). For TG analysis, samples
139 were placed in 100 μ L open aluminium pans under a dry air flow of 50 mL/min. The ramp of temperature
140 was from 50 to 600°C at 10°C/min. DSC measurements were done under the same conditions. The DSC
141 and TG curves indicate the resistance of SOM to thermal oxidation in air (Dell'Abate et al. 2002;
142 Fernández et al. 2011). Differential thermogravimetry (DTG) determines SOM fractions with differing
143 resistance to oxidation as defined by the temperatures at the maxima of the different combustion peaks.
144 The integral of DSC curves yields the heat of combustion/volatilization of SOM (Q_{SOM}) in the soils in
145 kJ/g OM or kJ/g C that is associated with the nature of the SOM. TG and DSC curves give the T50-TG
146 and T50-DSC of SOM defined as the temperature at which 50 % of the SOM mass and 50 % of the SOM
147 energy is lost during the combustion. A higher T50 temperature indicates higher thermal stability. These
148 properties are used to help in the interpretation of the calorespirometric ratios.

149 Calorespirometric measurements

150 SOM degradation rates through microbial metabolism were determined by calorespirometry with a TAM
151 III (TA Instruments) with six channels. Three aliquots of 1g from the 10 g subsamples being incubated
152 after rewetting were sealed into 4ml stainless steel ampoules and placed in the calorimeter. A vial of 0.4M
153 NaOH was introduced into some of the ampoules to measure the sum of the metabolic heat and CO₂
154 reaction rates. The procedure for the simultaneous measurement of heat and CO₂ rates is explained in
155 detail in previous papers (Barros et al. 2010; Barros et al. 2011; Barros et al. 2014a) and has been recently
156 reviewed (Wadsö and Hansen, 2015). Our procedure is based on the method developed by Hansen,
157 Criddle and coworkers (Criddle et al. 1990; Criddle et al. 1991) and considered up to now as the best
158 procedure to measure CO₂ and heat concomitantly by calorimetry. The pre-treatment of the samples is
159 adapted to get the best reproducibility with the type of calorimeter used in this work. Six samples were
160 run at the same time in each set of experiments and each experiment takes 48 hours. Four ampoules of
161 the six are used to measure the heat rate and two ampoules with NaOH are used to measure CO₂ rates.
162 The heat rate (ϕ_R in microwatts or μ J/second) is obtained from the ampoules without NaOH, and the CO₂
163 rate (R_{CO_2} in picomoles of CO₂ per second) is determined from the difference between the heat rates from
164 ampoules with NaOH and those without. This difference in heat rates is divided by the enthalpy change
165 for reaction of CO₂ with the NaOH solution, -108.5 kJ/mole, to obtain R_{CO_2} .

166 Calorespirometric measurements were recorded continuously for 48 hours. During the first 24 hours, the
167 heat derived from metabolism and the reaction between CO₂ and NaOH is recorded. Then the NaOH vial
168 is removed, the soil sample is reinserted in the calorimeter, and the recording continued for another 24
169 hours to check the reproducibility of ϕ_R in the six soil aliquots being measured at the same time. ϕ_R and
170 R_{CO₂} rates during the calorimetric measurements are plotted versus time to verify these rates are constant
171 and thus establish that there is no net growth. Then, the ϕ_R and CO₂ rates are plotted versus the 24 h of
172 measurement and the curves modeled as reported in previous papers (Barros et al. 2010; Barros et al.
173 2011). These plots are then integrated to yield the total heat released per gram of soil per day (R_q in J g⁻¹d⁻¹)
174 and the total CO₂ released in the same interval of time (R_{CO₂}) in $\mu\text{mol CO}_2 \text{ g}^{-1}\text{d}^{-1}$. Then, R_q is divided
175 by R_{CO₂} to yield the averaged calorespirometric ratio (R_q/R_{CO_2}) obtained during the measurement. The
176 quantities obtained for the heat and CO₂ released can be given also per hour instead of per day. It is
177 important the heat and CO₂ rates be measured over exactly the same period of time and concomitantly to
178 assure that the heat and CO₂ quantities are in phase and thus represent exactly the same period of
179 measurement. Calculations of these ratios from independent measurements of CO₂ and heat or over
180 different intervals of time for the heat than for the CO₂ can affect the values obtained for the
181 calorespirometric ratios. R_q/R_{CO_2} ratios are given in kJ/mol CO₂. CO₂ and heat rates were also normalized
182 to the C content of the samples to examine soil biological stability (Plante et al. 2011).

183 ¹³C CPMAS NMR

184 Some of the samples from the chronosequences were studied previously by ¹³C CPMAS NMR (Perez-
185 Cruzado et al. 2014). This method was also applied in this study to the chronosequence under *Eucalyptus*
186 *nitens* to provide additional data about the chemical state of C in SOM. The obtained spectra were
187 manually phased, baseline corrected and integrated with MestreNova software (*Mestrelab Research inc*).
188 For integration the spectra were divided into four regions representing different chemical environments of
189 a ¹³C nucleus: Alkyl C (0-45 ppm), O-Alkyl C (45-110 ppm), aromatic C (110-160 ppm), and carbonyl C
190 (160-210 ppm) to give the percentage of contribution of those groups to total SOM. The ratio of alkyl C
191 region intensity (0-45 ppm) to O-alkyl C region intensity (45-110 ppm) (A/O-A) was determined as
192 suggested by Baldock and Preston (1995). This ratio is considered an indicator of the extent of
193 decomposition and/or substrate quality for microbes. The aromaticity was determined by the equation
194 proposed by Hatcher et al. (1981) to assess the extent of SOM humification (Dai et al. 2001). These data

195 were provided for the afforested samples at the end of the rotation and compared with those of the pasture
196 and forest references.

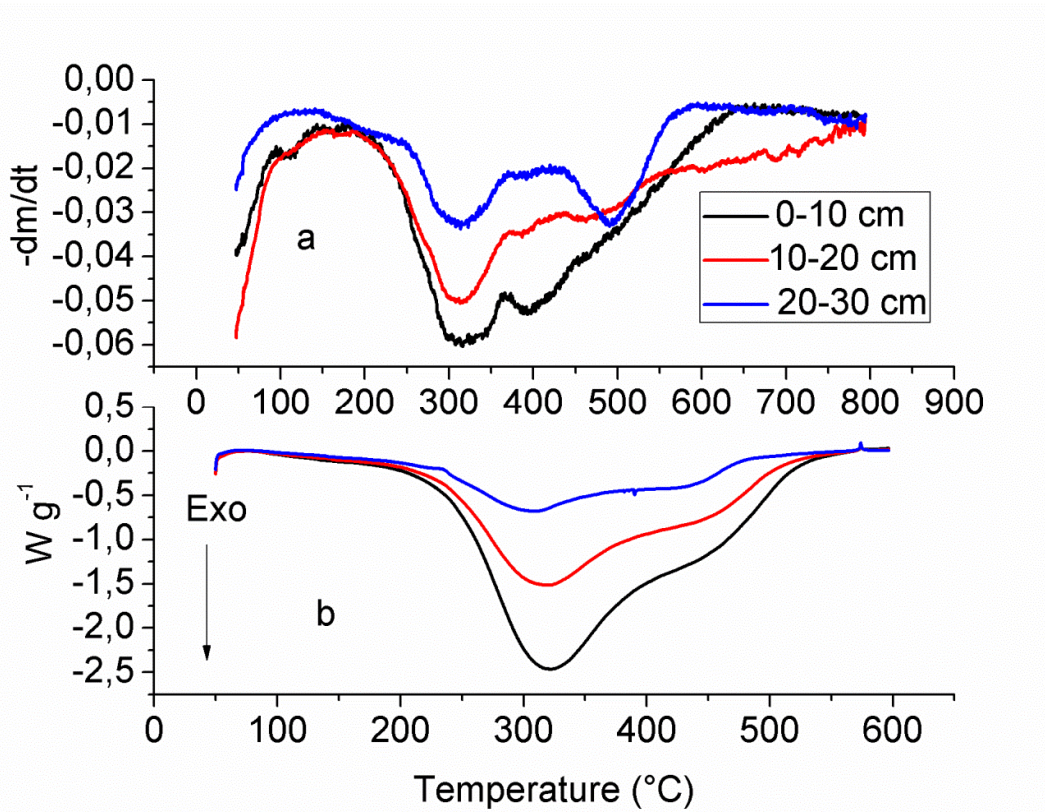
197 Statistical analyses

198 The influence of humidity on the biodegradation rates at each depth was tested by one way ANOVA.
199 Comparisons of R_q , R_{CO_2} and R_q/R_{CO_2} among soil samples sieved at different mesh sizes and among
200 samples from chronosequences were done as the average of the triplicates (three aliquots of 1 g from soil
201 incubated) with the standard deviation.

202 **3. Results**

203 3.1 Dependence of calorespirometric ratios on soil depth and humidity

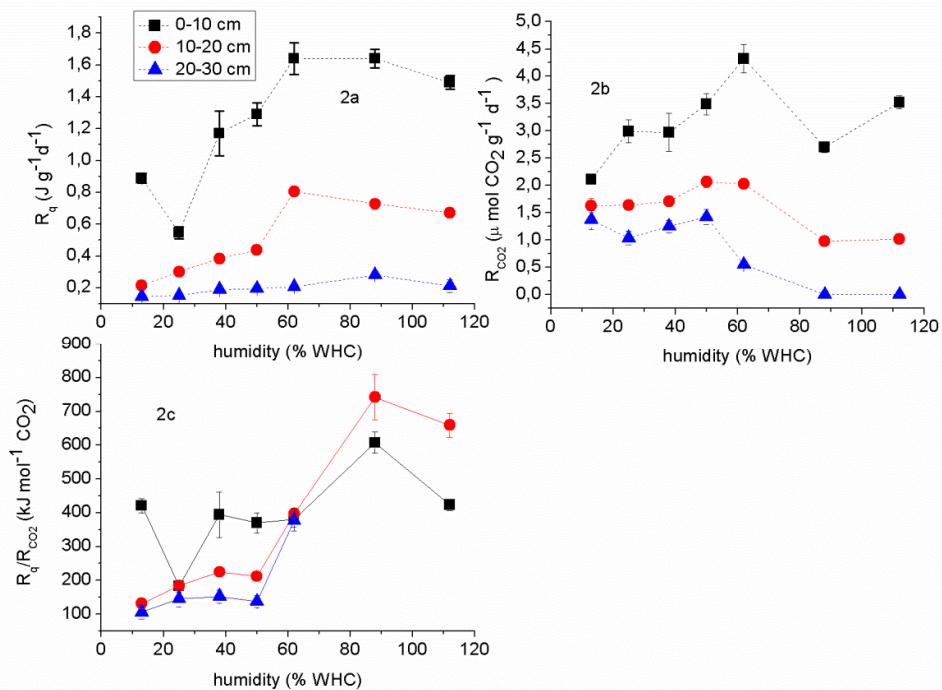
204 DTG and DSC curves in Figures (1a and 1b) show the SOM thermal properties and demonstrate that the
205 thermal stability of SOM changes markedly with depth. In all three samples, the maximum rates of mass
206 loss occur at the same three temperatures, T1 316°C, T2 395°C and T3 485°C defining three exothermal
207 fractions named Exo1, Exo2 and Exo3. Compared with the 0-10 cm sample, in the 10-20 cm sample, the
208 Exo2 fraction at 395°C is much smaller and the Exo3 fraction at 485°C is larger. At 20-30 cm, the 395°C
209 peak is almost absent and the peak at 495°C is much larger. The quantitative values for these thermal
210 SOM fractions are shown in table 1 together with analytical data on the samples. T50-TG was
211 significantly higher in the deepest sample than in the medium and upper layers (table 1), indicating that
212 SOM in the deepest sample is more thermally stable than SOM in the upper layers. The TG data indicate
213 the thermostability of SOM did not differ markedly between the upper and middle layers. Since there was
214 no significant change in the C/N ratio with depth, this cannot account for these differences.



215

216 DSC curves of the same samples are shown in Figure 1b. The DSC curves for all three samples have two
 217 peaks that are unresolved. Peak maxima occurred at the same temperature in the upper and middle
 218 samples, (321 and 449°C) but T1 and T2 were lower in the deepest sample (310 and 425°C) suggesting
 219 the SOM in this sample differs from the upper two samples. DSC data also indicated a change in the
 220 chemical nature of SOM with depth, i.e., T_{50-DSC} and Q_{SOM} decreased with soil depth as shown in table
 221 2.

222 Figure 2 shows the evolution of R_q , R_{CO_2} and R_q/R_{CO_2} with depth at differing humidity. R_q and R_{CO_2}
 223 decrease with soil depth as a consequence of the C and SOM depletion. ANOVA showed the variation of
 224 R_q and R_{CO_2} with humidity was significant in all soil layers.



225

226 In all samples, R_q and R_{CO_2} decrease with depth and increase with increasing humidity up to 62% of
 227 WHC (Figures 2a and 2b), above which R_q and R_{CO_2} values decreased. Inhibition of the biodegradation
 228 rates is stronger in the CO_2 rates than in the heat rates, indicating that biodegradation dissipates less CO_2
 229 at humidity above 62%. In the deepest soil layer at 88 and 112% of WHC, CO_2 production is completely
 230 inhibited, but the heat rate is still significantly above zero. As a consequence of the different effects on R_q
 231 and R_{CO_2} , humidity also affects the calorespirometric ratios, Figure 2c. At and below 50% humidity,
 232 calorespirometric ratios decline with increasing soil depth, but increase in all samples when humidity is
 233 higher than 62% in the 0-10 cm sample and higher than 50% in the 10-20 and 20-30 cm samples. Note
 234 that the calorespirometric ratios at 62% WHC are all near Thornton's constant (455 kJ/mol CO_2)
 235 indicating cellulose is probably the substrate.

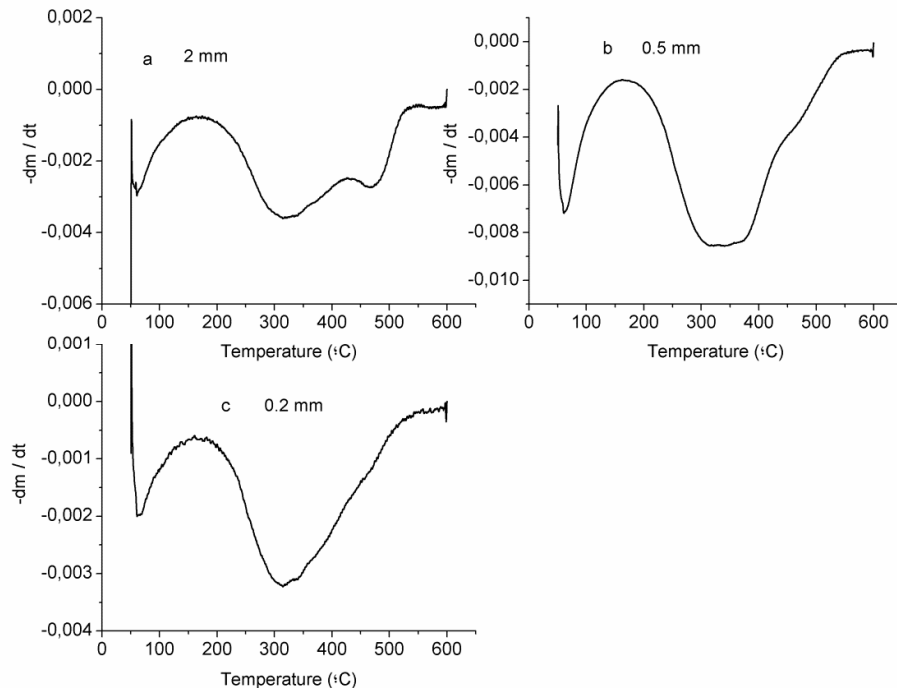
236

237 3.2 Influence of soil particle size

238

239 The DTG curves in Figure 3 indicate changes in the thermal properties of the SOM fractions obtained by
 240 sieving soil through different mesh sizes. Results of analyses and the thermal indices from DSC and TG

241 curves are shown in table 3. The lowest SOM value, which is found in the 2 mm fraction, is explained by
242 the presence of coarse mineral material.



243
244 As the particle size decreases, the fraction decomposing at T1 (Exo1) increasingly predominates over that
245 decomposing at T2 (Exo2). The Exo2 fraction is practically absent at the smallest particle size. The
246 decrease in TG-T50 with decreasing particle size indicates an evolution to lower thermal stability. The
247 DSC-T50 and Q_{SOM} also indicated changes in the chemical nature of the SOM in the soil fractions, but
248 without any clear trend.

249

250 R_q and R_{CO_2} are higher in the <0.5 and <0.2 mm fractions than in the 2 mm fraction (Table 3) because
251 more inactive inorganic material is present in the larger particles. Calorespirometric ratios also increased
252 with decreasing particle size, Table 3.

253

254 3.3 Differing soil management: effect of afforestation and tree species.

255

256 SOM biodegradation was tracked in two soil chronosequences from the northwest of Spain representing
257 the conversion from pasture to forestry. Soil samples were collected in stands afforested with *Pinus*

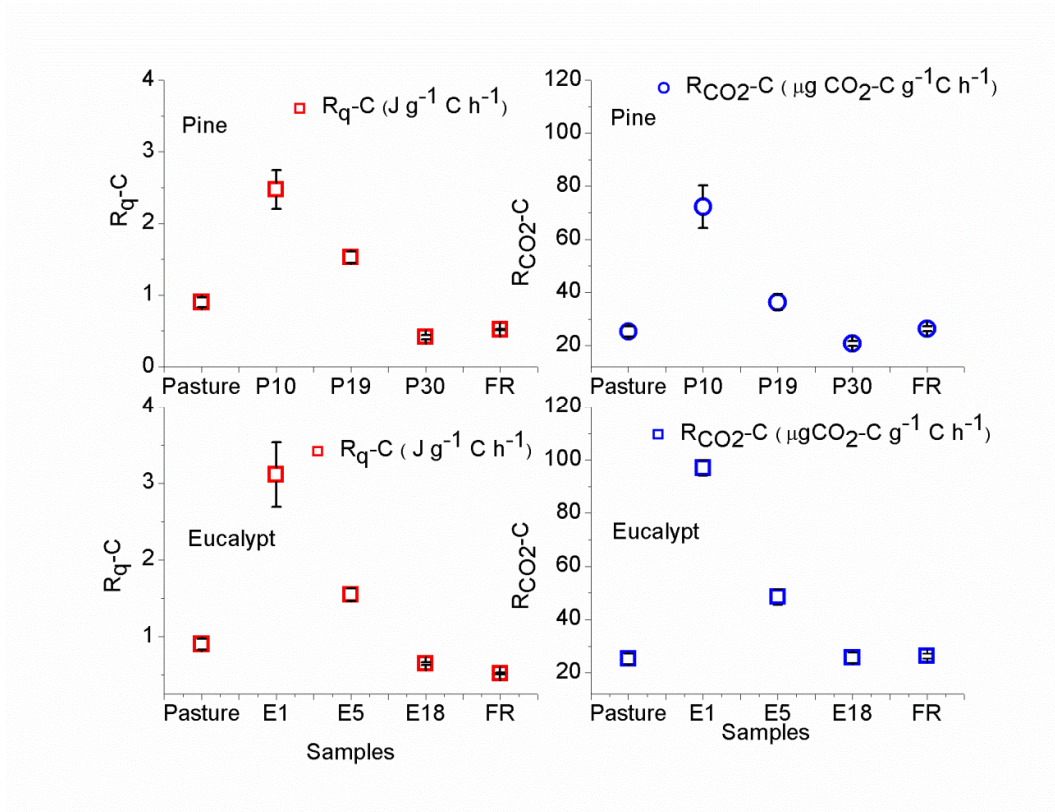
258 *radiata* and *Eucalyptus nitens*. Soil samples under eucalypt and pine showed an initial depletion of C
259 content during the first 5 years after afforestation in eucalypt stands and during 10 years after
260 afforestation in pine stands (Table 4). At the end of the rotation, samples from the eucalypt and pine
261 stands had a C content slightly higher than in the pasture reference and lower than the forest reference.
262 When soil C increased above that in the pasture, the T50-DSC values were higher than the pasture
263 reference, indicating that the SOM gained is more thermally stable than the pasture reference, but less
264 thermally stable than the forest reference.

265

266 Table 5 shows the results of analysis of the ^{13}C -CPMAS spectra. Afforested samples at the end of the
267 rotation had a higher degree of SOM microbial degradation, as indicated by the A/OA ratio, than the
268 pasture reference and lower or similar A/OA ratio than the forest reference. Aromaticity of the SOM also
269 tended to increase after conversion of pasture to pine forest. Contribution of O-Alkyl C mainly in
270 carbohydrates is higher in the pasture than in the forest sites at the end of the rotation.

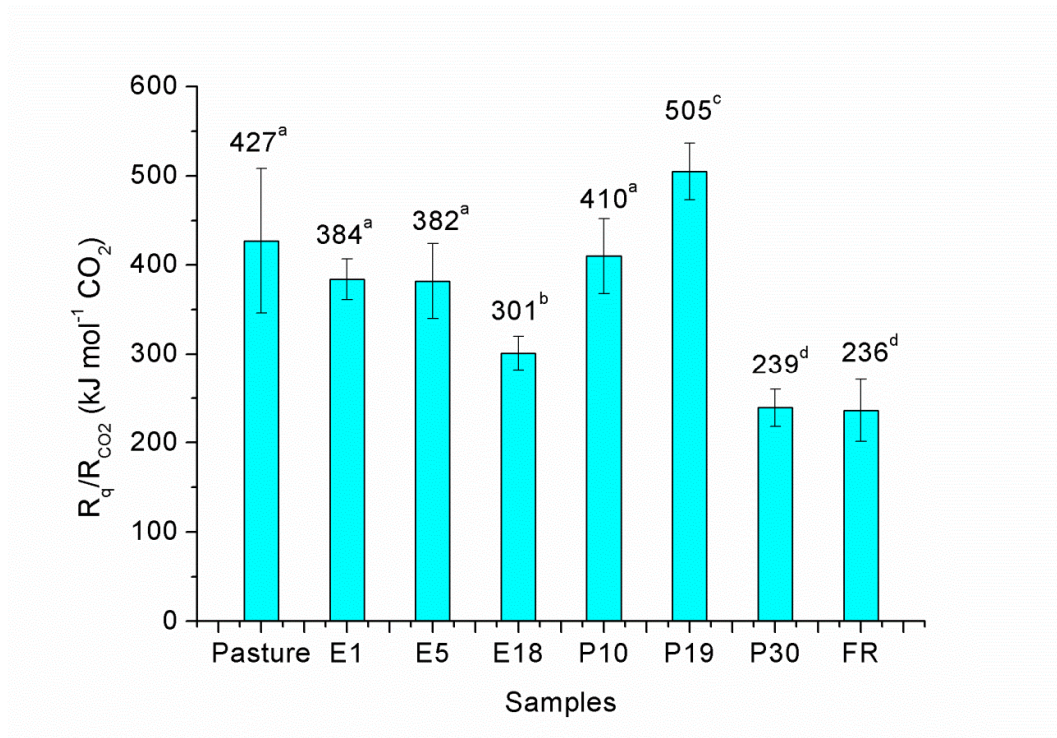
271

272 R_q and R_{CO_2} normalized to the soil C content along the chronosequences are shown in Figure 4. Evolution
273 of both rates was similar in both chronosequences. During the C loss period, stability against biological
274 degradation decreased in both eucalypt and pine stands. However, stability against biological degradation
275 increased during the C gain. At the end of the rotation, the biological stability of the samples was close to
276 that of the forest reference and higher than that of the pasture. Biological stability at the end of the
277 rotation was higher in the pine stand than in the eucalypt stand.



278

279 R_q/R_{CO_2} ratios along both chronosequences are shown in figure 5 together with those of the pasture and
 280 the forest reference. R_q/R_{CO_2} values were similar in the pasture, two youngest eucalypt stands and the
 281 youngest pine stand. R_q/R_{CO_2} ratios in the oldest eucalypt and pine stands differ markedly from each other
 282 and from all other samples. R_q/R_{CO_2} value in the oldest pine stand (P30) is significantly smaller than in the
 283 pasture and younger stands, and close to that of the forest reference.



284

285

286

287 4. Discussion

288 R_q/R_{CO_2} ratios were in the range predicted by equation 1 in the soil size fractions, in the samples from the
 289 chronosequences, and in the 0-10 cm samples with humidity from 13 to 62% of WHC, see Table 1.

290 Nevertheless, some of the soil treatments explored here yielded R_q/R_{CO_2} values higher and lower than
 291 those expected from equation 1. Table 6 summarizes the possible reactions in soil giving R_q/R_{CO_2} values
 292 higher than 611 kJ/mol and lower than 228 kJ/mol.

293 The R_q/R_{CO_2} values in Table 3 for R_q/R_{CO_2} 0-10 cm topsoil under *Pinus radiata* show that mechanical
 294 fractionation has little effect on metabolic pathways, and the values indicate the primary reaction is
 295 decarboxylation (see Table1) that typically involves carboxylic acids and the citric acid cycle, as well as
 296 biosynthetic oxidation of amino-acids to amines. The observed evolution of thermal properties and
 297 biodegradation rates (figure 3 and Table 3) with particle size also suggest the R_q/R_{CO_2} values of these
 298 fractions involve decarboxylation reactions in the respiration of labile substrates like carbohydrates.

299 The Exo 1 considered as labile OM (Grisi et al. 1998; Dell'Abate et al. 2002; Lopez-Capel et al. 2005)
300 increased and the TG-T50 value decreased as the mesh size decreased suggesting protection of labile
301 SOM within micro and macro aggregates (Six et al. 2002; Chenu et al. 2009). The nature of the SOM
302 protected within aggregates may be highly dependent on the soil type and environmental conditions (Six
303 and Paustian, 2014). In this study, labile forms of SOM are released when macroaggregates are crushed,
304 making substrates more available to microbial degradation. This can explain the changes in the
305 biodegradation rates as the mesh size decreases.

306

307 All of the R_q/R_{CO_2} values determined in the soils from the chronosequences are within the range predicted
308 by equation 1, see figure 5. The value of R_q/R_{CO_2} in the pasture, 427 kJ/mol, indicates the metabolism is
309 largely oxidative respiration of cellulose and/or humic substances. The value of R_q/R_{CO_2} in the forest
310 reference, 236 kJ/mol, indicates the metabolism is largely oxidative decarboxylation of products from
311 earlier partial oxidation of carbohydrates and/or humates. SOM properties from the chronosequences
312 were determined only by DSC and ^{13}C CPMAS. T50-DSC generally increased after afforestation at the
313 end of the rotation (Pérez-Cruzado et al. 2014). In the two chronosequences in this study, there were no
314 remarkable changes in T50-DSC with respect to that of the pasture precursor in the young forest stands
315 (E1 and E5 years in the eucalypt stands and P10 and P19 years in the pine stands). Microbial degradation
316 rates per unit soil C (figure 4) are the highest in the young forest sites, indicating the lowest biological
317 stability of SOM, which explains the C loss during the first years after the land use change. R_q/R_{CO_2}
318 values in these forest sites are not significantly different than that of the pasture reference. T50-DSC
319 increased in the oldest afforested sites (E18 and P30), associated with C gain, lower microbial
320 degradation rates per unit of soil C, and thus, higher biological stability. Higher thermal stability is
321 generally associated with higher recalcitrance and physical SOM stabilization (Plante et al. 2011; Peltre et
322 al. 2014). The ^{13}C CPMS results showed aromaticity increases and the carbohydrate contribution to total
323 C decreases in the oldest forest stands and in the forest reference compared to that in the pasture. These
324 thermal and chemical properties of SOM from pasture, young and mature forests agree with those
325 reported recently by similar studies describing more labile nature of SOM in pastures and young forests
326 than in mature forests (Guidi et al. 2014). Here, those changes in SOM are accompanied by a significant
327 decrease in R_q/R_{CO_2} in the oldest afforested sites to 301 kJ/mol in the Eucalypt stand (E18) and to 239
328 kJ/mol in the Pine stand (P30) approaching to the value in the mature forest reference (FR:236 kJ/mol).

329 Evolution in the R_q/R_{CO_2} values denotes the change in the nature of SOM along the chronosequences. As
330 the forest ecosystem evolves, R_q/R_{CO_2} quantitative values follow the trend: Pasture > *Eucalypt nitens* >
331 *Pinus radiata* in the mature forests. This trend is very similar to that reported for a different Pine
332 chronosequence in the same area (Barros et al. 2014). The R_q/R_{CO_2} values are also close to those reported
333 in a previous paper for soil samples with similar C contents and soil properties under pasture (566 ± 61
334 kJ/mol CO_2), pine (269 ± 8 kJ/mol CO_2) and eucalypt (272 ± 19 kJ/mol CO_2) in the north of Spain (Barros
335 et al. 2011). Other R_q/R_{CO_2} values reported in Barros et al. (2011) were from sites located at longer
336 distances from the ones reported here and represent soils and possibly microbes with different properties.
337 The same decrease in R_q/R_{CO_2} in forest soils compared with grasslands has been recently reported by
338 other authors (Herrmann and Bölscher, 2015). R_q/R_{CO_2} ratios are clearly sensitive to the SOM evolution
339 from pasture to forest and seem reproducible within a given ecosystem. More labile SOM yields R_q/R_{CO_2}
340 values indicating metabolism of cellulose, lignin and proteins, mainly in pastures and young forests, while
341 mature forests show a metabolism based on decarboxylation of products from earlier partial oxidation of
342 carbohydrates and/or humates. In our samples this trend in R_q/R_{CO_2} ratios accompanied the depletion in
343 the contribution of carbohydrates to total C. More research will be needed to assess effects of soil type
344 and microorganism species.

345

346 Thermal properties showed evolution of SOM towards a more thermally stable state as soil depth
347 increases, compatible with the reported evolution of SOM with depth to a more recalcitrant and stable
348 state (Fierer et al. 2003; Marinari et al. 2010). This should make a more negative γ_s in equation 1 that
349 predicts increasing R_q/R_{CO_2} ratios with depth, but R_q/R_{CO_2} ratios tended to decrease below 228 kJ/mol as
350 soil depth increases when humidity ranges from 13 to 62 % of WHC. This occurs if CO_2 is being
351 liberated by processes with a smaller enthalpy change than that for oxidation of SOM by O_2 (455 kJ/mol).
352 Some examples that occur in soils are when organic matter reacts with carbonates and bicarbonates of the
353 soil mineral fraction and when metal oxides serve as electron acceptor if soil O_2 is low (Lovley et al.
354 1996; Hansel et al. 2003; Borch et al. 2010). For example, reaction with ferrihydrite, the most common
355 mineral in soil (Sadeghi et al. 2015), produces only about 1% of the heat released by the reaction of the
356 same organic matter with O_2 . These processes are common in soils by Fe-metabolizing bacteria (Byrne et
357 al. 2015). Anaerobic metabolism in general also produces low R_q/R_{CO_2} ratios because the enthalpy change
358 is small. Samples from 10-20 and 20-30 cm were the samples yielding R_q/R_{CO_2} ratios too low to be

359 explained by equation 1. Those samples are rich in recalcitrant organic matter and have an acid pH (4.50);
360 thus oxidation of the organic matter through metal oxides could explain the low R_q/R_{CO_2} ratios obtained.
361 SOM from the sampling region are reported to be rich in Al-humus and Fe-humus complexes (Rodríguez-
362 Lado ,2014). These issues complicate the interpretation of R_q/R_{CO_2} ratios, but do not invalidate their use
363 to provide more information about the nature of the SOM reactions. The R_q/R_{CO_2} evolution with depth
364 clearly indicates a change in the type of microbial metabolism involving C mineralization from the soil
365 surface to the deepest soil layers as pointed out by other authors (Pothoff et al. 2006). Comparison with
366 other soil types would deserve more attention.

367 Humidity percentages higher than 62% of WHC yielded R_q/R_{CO_2} ratios too large to be explained by
368 equation 1. R_q/R_{CO_2} ratios higher than 611 kJ/mol occur either because CO_2 is not being produced or
369 because it is not being measured. Oxidation by O_2 does not always produce CO_2 in soil as in the case of
370 lignin and humates because of the presence of dihydroxy aromatics that are readily oxidized to quinones.
371 The electrons from the reducing agent go through the electron transport chain in the cell and O_2 is the
372 electron acceptor but no CO_2 is produced. In the second case, CO_2 is being produced but not measured
373 because it can be trapped by acid-base reactions in the soil. This problem occurs with basic soils (which is
374 not the case here) and if organisms such as algae that sequester CO_2 are present. If excess liquid is
375 present, as the case here, dissolved CO_2 could be very slow to be released. The results indicate that
376 different microorganisms are involved in the immediate response of soil to water addition at different
377 depths and that different metabolic paths can be identified by this procedure.

378 In conclusion, variations in R_q/R_{CO_2} ratios indicate changes in the biochemistry of soil samples and yield
379 more information about C dynamics than CO_2 rates or SOM physical properties alone. Data on R_q/R_{CO_2}
380 ratios is a novel alternative to evaluate the biochemical paths for carbon mineralization in different
381 ecosystems and deserves more investigation.

382

383

384 **Acknowledgments:** This work was funded by the project of Xunta de Galicia (10PXIB291027PR). ^{13}C
385 CPMAS analysis were done by M. Martín Pastor in the NMR services of the University of Santiago de
386 Compostela (RIAIDT).

387

388 **References**

389 Baldock, J.A., Preston, C.M., 1995. Chemistry of carbon decomposition processes in forests as revealed
390 by solid-state carbon-13 nuclear magnetic resonance. In: McFee, W.W., Kelly, J.M. (Eds), Carbon Forms
391 and Functions in Forest Soils. Soil Science Society of America, Madison, WI, pp. 89–117.

392 Barros, N., Feijoo, S., 2003. A combined mass and energy balance to provide bioindicators of soil
393 microbiological quality. *Biophysical Chemistry* 104(3), 561-572.

394 Barros, N., Salgado, J., Feijóo, S., 2007. Calorimetry and soil. *Thermochimica Acta* 458, 11-17.

395 Barros, N., Salgado, J., Rodríguez-Añón, J.A., Proupín, J., Villanueva, M., 2010. Calorimetric
396 approach to metabolic carbon conversion efficiency in soils: Comparison of experimental and theoretical
397 models. *Journal of Thermal Analysis and Calorimetry* 99, 771-777.

398 Barros, N., Feijoo, S., Hansen, L.D., 2011. Calorimetric determination of metabolic heat, CO₂ rates and
399 the calorespirometric ratio of soil basal metabolism. *Geoderma* 160, 542-547.

400 Barros, N., Merino, A., Martín-Pastor, M., Pérez-Cruzado, C., Hansen, L., 2014. Changes in soil
401 organic matter in a forestry chronosequence monitored by thermal analysis and calorimetry. *Spanish*
402 *Journal of Soil Science*. DOI: 10.3232/SJSS.2014.V4.N3.02.

403

404 Battley, E.H., 2013. A theoretical study of the thermodynamics of microbial growth using *saccharomyces*
405 *cerevisae* and a different free energy equation. *The Quaterly Review of Biology* 88, 69-96.

406 Borch, T., Kretzschma, R., Kapple,r A., Cappellen, P. V., Ginder-Vogel, M., Voegelin, A., Campbell,
407 K., 2010. Biogeochemical redox processes and their impact on contaminant dynamics. *Environmental*
408 *Science and Technology* 44,15-23.

409 Byrne, J. M., Klueglein, N., Pearce, C., Rosso, K. M., Appel, E., Kappler, A., 2015. Redox cycling of
410 Fe(II) and Fe (III) in magnetite by Fe-metabolizing bacteria. *Science* 347, 1473-1476.

411

412 Chenu, C., Virto, J., Plante, A.F., Elsass, F., 2009. Clay-size organo-mineral complexes in temperate
413 soils: relative contributions of sorptive and physical protection. In: Laird, A., Cervini-Silva, J., (Eds),
414 CMS workshop lectures. The Clay Minerals Society, pp. 120-135.

415 Conant, R.T., Ryan, M.G., Agren, H.E., Birge, E.A., Davidson, P.E., Eliason et al., 2011. Temperature
416 and soil organic matter decomposition rates: Synthesis of current knowledge and a way forward. *Global*
417 *Change Biology* 17, 3392-3404.

418 Criddle, R. S., Breindenbach, R. W., Rank, D. R., Hopkin, M. S., Hansen, L. D., 1990. Simultaneous
419 calorimetric and respirometric measurements on plant tissues. *Thermochimica Acta* 172, 213-221.

420 Criddle, R. S., Breindenbach, R. W., Hansen, L. D., 1991. Plant calorimetry: how to quantitatively
421 compare apples and oranges. *Thermochimica Acta* 193, 67-90.

422 Dai, X.Y., Ping, C.L., Candler, R., Haumaier, L., Zech, W., 2001. Characterization of Soil Organic
423 Matter Fractions of Tundra Soils in Artic Alaska by Carbon-13 Nuclear Magnetic Resonance
424 Spectroscopy. *Soil Science Society of America Journal* 65, 87-93.

425 Dell'Abate, M.T., Benedetti, A., Trinchera, A., Dazzi, C., 2002. Humic substances along the profile of
426 two typic haploxerert. *Geoderma* 107,281-296.

427

428 Fernández, J. M., Plante, A. F., Leifeld, J., Rasmussen, C., 2011. Methodological considerations for
429 using thermal analysis in the characterization of soil organic matter. *Journal of Thermal Analysis and*
430 *Calorimetry* 104,389-398.

431 Field, C.B., Lobell, D.B., Peters, H.A., Chiariello, N.R., 2007. Feedbacks of terrestrial ecosystems to
432 climate change. *Annual Review of Environmental Resources*. 32, 1-29.

433 Fierer, N., Schimel, J.P., Holden, P.A., 2003. Variations in microbial community composition
434 through two soil depth profiles. *Soil Biology and Biochemistry* 35,167-176.

435

436 Grisi, B., Grace, C., Brookes, P.C., Benedetti, A., Dell'Abate, M.T., 1998. Temperature effects on
437 organic matter and microbial Biomass dynamics in temperate and tropical soils. *Soil Biology and*
438 *Biochemistry* 30,1309-1315.

439

440 Guidi, C., Vesterdal, L., Cannell, D., Leifeld, J., Gianelle, D., Rodeghiero, M., 2014. Carbohydrates and
441 Thermal analysis reflects changes in soil organic matter stability after forest expansion on abandoned
442 grassland. *Geophysical Research Abstracts Vol 16 EGU2014-7267*.

443

444 Hansel, C. M., Benner, S. G., Neiss, J., Dohnalkova, A., Kukkadapu, R. K., Fendorf, S., 2003. Secondary
445 mineralization pathways induced by dissimilatory iron reduction of ferrihydrite under advective flow.
446 *Geochimica and Cosmochimica Acta* 67, 2977-2992.

447

448 Hansen, L.D., Macfarlane, C., McKinnon, N., Smith, B.N., Criddle, R.S., 2004. Use of calorimetric
449 ratios, heat per CO₂ and heat per O₂, to quantify metabolic paths and energetics of growing cells.
450 *Thermochimica Acta* 422, 55-61.

451 Harris, J.A., Ritz, K., Coucheney, E., Grice, S.M., Lerch, T.Z., Pawlett, M., Herrmann, A.M., 2012. The
452 thermodynamic efficiency of soil microbial communities subject to long-term stress is lower than those
453 under conventional input regimes. *Soil Biology and Biochemistry* 47, 149-157.

454 Hatcher, P.G., Schnitzer, M., Dennis, L.W., Maciel, G.E., 1981. Aromaticity of humic substances in
455 soils. *Soil Science Society of America Journal* 45, 1089-1094.

456 Herrmann, A., Coucheney, E., Nunan, N., 2014. Isothermal calorimetry provides new insight into
457 terrestrial carbon cycling. *Environmental Science and Technology*. doi: 10.1021/es403941h.

458 Herrmann, A. M., Bölscher, T., 2015. Simultaneous screening of microbial energetics and CO₂ respiration
459 in soil samples from different ecosystems. *Soil Biology and Biochemistry* 83, 88-92.

460 Hunt, A.P., Parry, J.D., Hamilton-Taylor, J., 2000. Further evidence of elemental composition as an
461 indicator of the bioavailability of humic substances to bacteria, *Limnology and Oceanography* 45(1), 237-
462 241.

463 IUSS Working Group WRB (2006) World reference base for soil resources 2006. *World Soil Resources*
464 *Reports* 626 No. 103. FAO, Rome.

465

466 Lopez-Capel, E., Sohi, S.P., Gaunt, J.L., Manning, D.A.C., 2005. Use of thermogravimetry–
467 differential scanning calorimetry to characterize modelable soil organic matter fractions. Soil Science
468 Society of America Journal 69,136–140.
469

470 Lovley, D. R., Coates, J. D., Blunt-Harris, E. L., Phillips, E. J. P., Woodward, J. C.,1996 Humic
471 substances as electron acceptors for microbial respiration. Nature 382, 445-448.

472 Marinari, S., Dell’Abate, M.T., Brunetti, G., Dazzi, C., 2010. Differences of stabilized organic carbon
473 fractions and microbiological activity along mediterranean Vertisols and Alfisols profiles. Geoderma 156,
474 379-388.

475 Matheson, S., Ellingson, D. J., Mc Carlie, V.W., Smith, B.N., Criddle, R.S., Rodier, L., Hansen,
476 L.D., 2004. Determination of growth and maintenance coefficients by calorespirometry. Functional Plant
477 Biology 31, 929-939.

478 Núñez-Regueira, L., Proupín-Castiñeiras, J., Rodríguez-Añón, J.A., Villanueva-López, M., Núñez-
479 Fernández, O., 2006. Design of an Experimental Procedure to Asses Soil Health. Journal of Thermal
480 Analysis and Calorimetry 85, 271-277.

481 Pérez-Cruzado, C., Mohren, G.M.J., Merino, A., Rodríguez-Soalleiro, R., 2012. Carbon balance for
482 different management practices for fast growing tree species planted on former pastureland in southern
483 Europe: a case study using the CO₂Fix model. European Journal of Forest Research 131, 1695–1716.

484 Pérez-Cruzado, C., Sande, B., Omil, B., Rovira, P., Martín-Pastor, M., Barros, N., Salgado, J.,
485 Merino, A., 2014. Organic matter properties in soils afforested with *Pinus radiata*. Plant and Soil 374,
486 381-398.

487 Peltre, C., Fernández, J.M., Craine, J.M., Plante, A.F., 2014. Relations between Biological and
488 Thermal Indices of Soil Organic Matter Stability Differ with Soil Organic Carbon Level. Soil Science
489 Society of America Journal. 77, 2020-2028.

490 Plante, A.F., Fernández, J.M., Leifeld, J., 2009. Application of thermal analysis techniques in soil
491 science. Geoderma 153, 1–10.

492 Plante, A.F., Fernández, J.M., Haddix, M.L., Steinweg, J.M., Conant, R.T., 2011. Biological, chemical
493 and thermal indices of soil organic matter stability in four grassland soils. *Soil Biology and Biochemistry*
494 43,1051-1058.

495 Potthoff, M., Steenwerth, K.L., Jackson, L.E., Drenovsky, R.E., Scow, K.M., Joergensen, R.G., 2006.
496 Soil microbial community composition as affected by restoration practices in California grassland. *Soil*
497 *Biology and Biochemistry* 38, 1851-1860.

498

499 Rodríguez-Añón, J.A., Proupín-Castiñeiras, J., Villanueva-López, M., Nuñez-Fernández, O., 2007.
500 Development of an experimental procedure to analyse the soil health state by microcalorimetry. *Journal*
501 *of Thermal Analysis and Calorimetry* 87, 15-19.

502 Rodríguez-Lado, L. 2014. Influence of climatic parameters in the carbon content of topsoils in Galicia
503 (NW Spain) *Geophysical Research Abstracts*, vol. 16: 13750, EGU General Assembly 2014.

504 Sadeghi, O., Zakharov, L. N., Nyman, M., 2015. Aqueous formation and manipulation of the iron-oxo
505 Keggin ion. *Science (AAAS)* 347, 1359-1362.

506 Six, J., Conant, R.T., Paul, E.A., Paustian, K., 2002. Stabilization mechanisms of soil organic matter:
507 Implications for C-saturation of soils. *Plant and Soil* 241, 155-176.

508 Six, J., Paustian, K., 2014. Aggregate-associated soil organic matter as an ecosystem property and a
509 measurement tool. *Soil Biology and Biochemistry* 68, A4-A9.

510 Wadsö, L., Li, Y., Bjurman, J., 2004. Measurements on two mould fungi with a calorimetric
511 method. *Thermochimica Acta* 422, 63-68.

512 Wadsö, L., Hansen, L., 2015. Calorespirometry of terrestrial organisms and ecosystems. *Methods* 76, 11-
513 19.

514

515

516

517 Tables

518 Table 1. Expected values of R_q/R_{CO_2} for substances found in soil organic matter.

| Substance | Oxidation number/ γ_s | $R_q/R_{CO_2}/ \text{kJ mol}^{-1}$ |
|-------------------|------------------------------|------------------------------------|
| Cellulose, starch | 0 | 455 |
| Lignin | -0.60 ± 0.06^a | 523 |
| Protein | -1.0 | 543 |
| Lipid | -1.4 | 611 |
| Humates | $-0.1 \text{ to } +0.9^b$ | 470 to 350 |
| Decarboxylation | +2 | 228 |

519 a. <http://terra.rice.edu/department/faculty/masiello/RIGG/html/research/cox.html>

520 b. Hunt et al. 2000.

521

522 Table 2: Soil elemental composition (Organic Matter, OM%; Carbon percentage, C%; carbon to nitrogen
523 ratio, C/N). TG fractions defined by the maximum temperatures in the DTG curves (Exo1, Exo2 and
524 Exo3), the temperatures of 50% mass loss (T50-TG) and 50% energy loss (T50-DSC), and the total
525 energy loss (Q_{SOM}).

| Samples depth | 0-10 cm | 10-20 cm | 20-30 cm |
|-------------------------|----------------|------------------|-----------------|
| OM (%) | 16.00 ± 1 | 12.54 ± 0.10 | 8.12 ± 0.77 |
| C (%) | 6.42 | 4.62 | 3.08 |
| Exo1 (%) | 48 ± 3 | 49 ± 4 | 56 ± 1 |
| Exo 2 (%) | 52 ± 3 | 17 ± 3 | 0 |
| Exo 3 (%) | 0 | 34 ± 3 | 44 ± 4 |
| C/N | 19 | 18 | 19 |
| T50-TG | 376 ± 2 | 375 ± 2 | 383 ± 3 |
| T50-DSC | 346 ± 2 | 339 ± 2 | 328 ± 3 |
| $Q_{SOM}(\text{kJ/gC})$ | 28.0 ± 0.2 | 24.0 ± 0.2 | 25.0 ± 0.2 |

526

527

528

529

530 Table 3: C%, OM%, thermal data, biodegradation rates (R_q and R_{CO_2}), and calorespirometric ratios
 531 (R_q/R_{CO_2}) of soil samples sieved at different mesh sizes.

| Fractions → | 2mm | <0.5 mm | <0.2 mm |
|---|-----------|------------|------------|
| C (%) | 3.80±0.04 | 8.21±0.24 | 7.80±0.08 |
| OM (%) | 8.64±0.35 | 20.67±0.20 | 15.73±0.09 |
| Exo 1 (%) | 71±1 | 86±1 | 100 |
| Exo 2 (%) | 29±1 | 14±1 | ND |
| TG-T50 (°C) | 358±2 | 345±1 | 339±1 |
| DSC-T50 (°C) | 345±1 | 354±3 | 343±2 |
| Q_{SOM} (kJ / g C) | 33±2 | 24±3 | 37±2 |
| R_q (mJ/g h) | 62±1 | 122±6 | 102±3 |
| R_{CO_2} ($\mu\text{molCO}_2/\text{g h}$) | 0.26±0.01 | 0.49±0.02 | 0.34±0.01 |
| R_q/R_{CO_2} (kJ/mol) | 238 ± 10 | 249 ± 16 | 300 ± 12 |

532

533

534

535

536

537

538

539

540

541

542 Table 4: Elemental and thermal properties of the soil chronosequences compared with those in the pasture
 543 and forest references. * Tree species. ** Data reported with permission of Springer Science+Business
 544 Media.

| Samples | Q / kJ g ⁻¹ | T1/°C | T2/°C | T50-DSC | C/ % | C/N |
|-----------------|------------------------|---------|---------|---------|------------|--------|
| Pasture | 1.69±0.04 | 319±1 | 375±2 | 336±2** | 8.00±0.15 | 15±0.3 |
| <i>Eucalypt</i> | | | | | | |
| <i>nitens*</i> | | | | | | |
| E1 | 1.47±0.06 | 322 ± 1 | 394 ± 1 | 337±1 | 6.74±0.44 | 12±1 |
| E5 | 1.15±0.01 | 325 ± 2 | 395 ± 2 | 349±2 | 5.18±0.34 | 10±1 |
| E18 | 1.45±0.03 | 328 ± 1 | ND | 348±1 | 9.15±0.60 | 12±1 |
| <i>Pinus</i> | | | | | | |
| <i>radiata*</i> | | | | | | |
| P10 | 0.59±0.01 | 310 ± 1 | 401±1 | 335±1** | 2.71±0.18 | 12±1 |
| P19 | 0.98±0.04 | 320 ± 1 | 424±1 | 345±1** | 4.45±0.29 | 13±1 |
| P30 | 2.14±0.01 | 318 ± 1 | 378±1 | 348±1** | 9.42±0.61 | 19±1 |
| FR | 2.18±0.02 | 328±1 | 377±2 | 366±2** | 11.57±0.30 | 26±1 |

545

546

547 Table 5: ¹³C-CPMAS Results. * Afforested samples at the end of the rotation. Data published with
 548 permission of Springer Science + Business Media.

549

| Samples | Alkyl C | O-AlkylC | AroC | CarbonilC | A/OA | Aromaticity |
|---------------------|---------|----------|------|-----------|------|-------------|
| Pasture | 24 | 52 | 19 | 5 | 0.46 | 0.20 |
| E18* | 25 | 48 | 18 | 9 | 0.52 | 0.20 |
| P30* | 26 | 38 | 27 | 9 | 0.68 | 0.30 |
| Forest Reference | 26 | 40 | 25 | 9 | 0.65 | 0.27 |

550

551

552

553 Table 6. Summary of reasons for observations in soil of R_q/R_{CO_2} values outside the range of equation 1
554 predictions.

| $R_q/R_{CO_2} > 611$ kJ/mol | $R_q/R_{CO_2} < 228$ kJ/mol |
|--|---|
| Reaction of O_2 with dihydroxy aromatics in lignin and humates | CO_2 is produced by a disproportionation reaction with $\Delta H \approx 0$ |
| CO_2 reacts with carbonates in basic soils | CO_2 is produced by reaction of organic acids with carbonates or bicarbonates in the soil |
| CO_2 is sequestered by algae | Metal oxides are the electron acceptor under low O_2 |
| CO_2 is dissolved in excess liquid water | Anaerobic metabolism because of low O_2 or other stresses |

555

556 Legends for the figures

557 Figure 1: DTG (1a) and DSC (1b) curves of the soil samples collected from different depths.

558 Figure 2: Plots of the heat and CO_2 rates (2a and 2b) together with the calorespirometric ratios (2c)
559 obtained at different humidity percentages in soil samples from different depths.

560 Figure 3: DTG curves of the different soil size fractions.

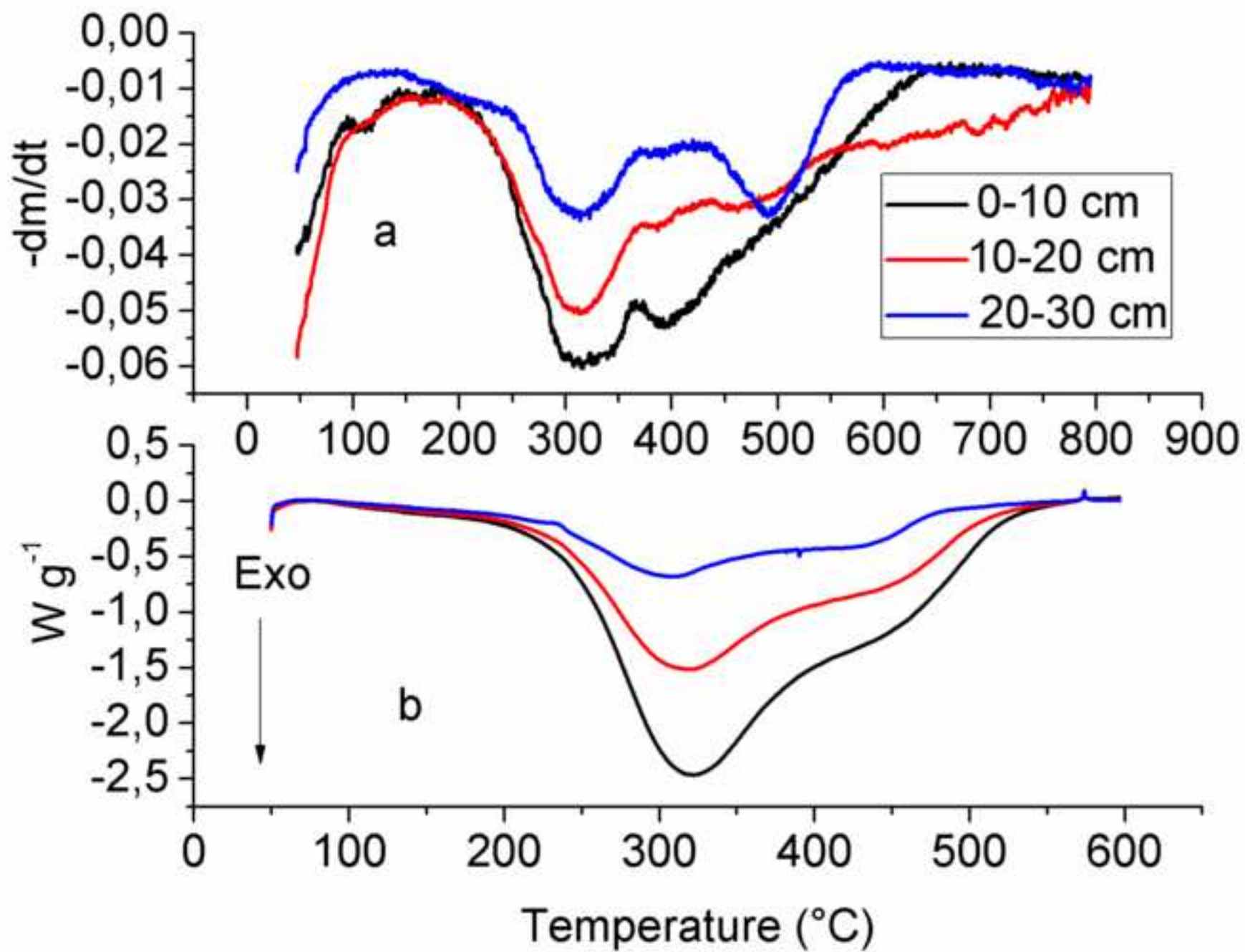
561 Figure 4: Evolution of the heat rate (R_q) and CO_2 rate (R_{CO_2}) normalized to the C content of the soil
562 samples along the chronosequences of *Eucalyptus nitens* and *Pinus radiata*.

563 Figure 5: Values of the calorespirometric ratios (R_q/R_{CO_2}) obtained along the chronosequences compared
564 with those in the pasture and forest references (FR).

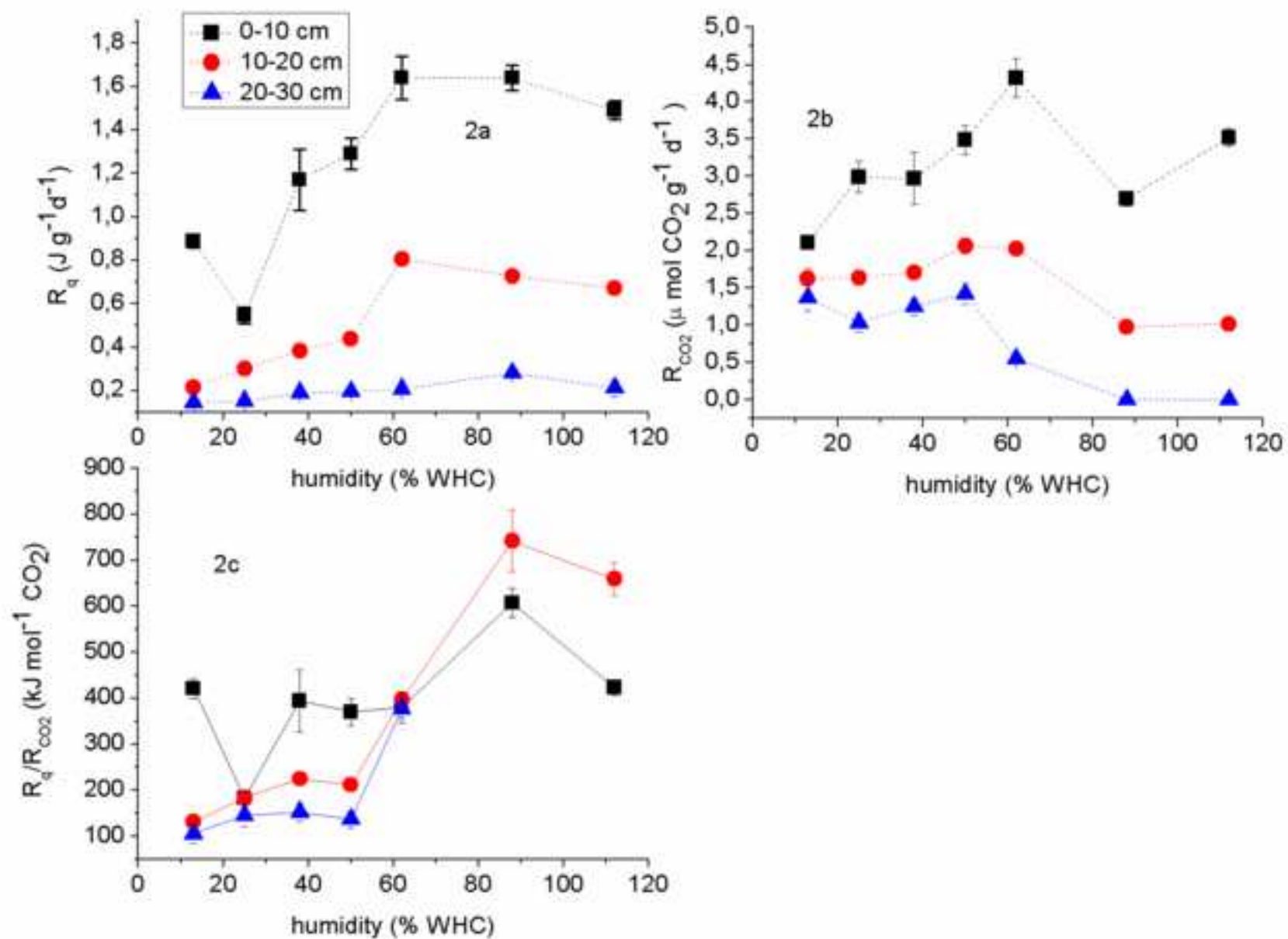
565 **a:** Samples with similar R_q/R_{CO_2} values to that of the pasture. **b:** R_q/R_{CO_2} differing from that in the pasture
566 in the Eucalypt stands. **c:** R_q/R_{CO_2} values higher than that in the pasture. **d:** R_q/R_{CO_2} values similar to that
567 in the forest reference

568

Figure
[Click here to download high resolution image](#)

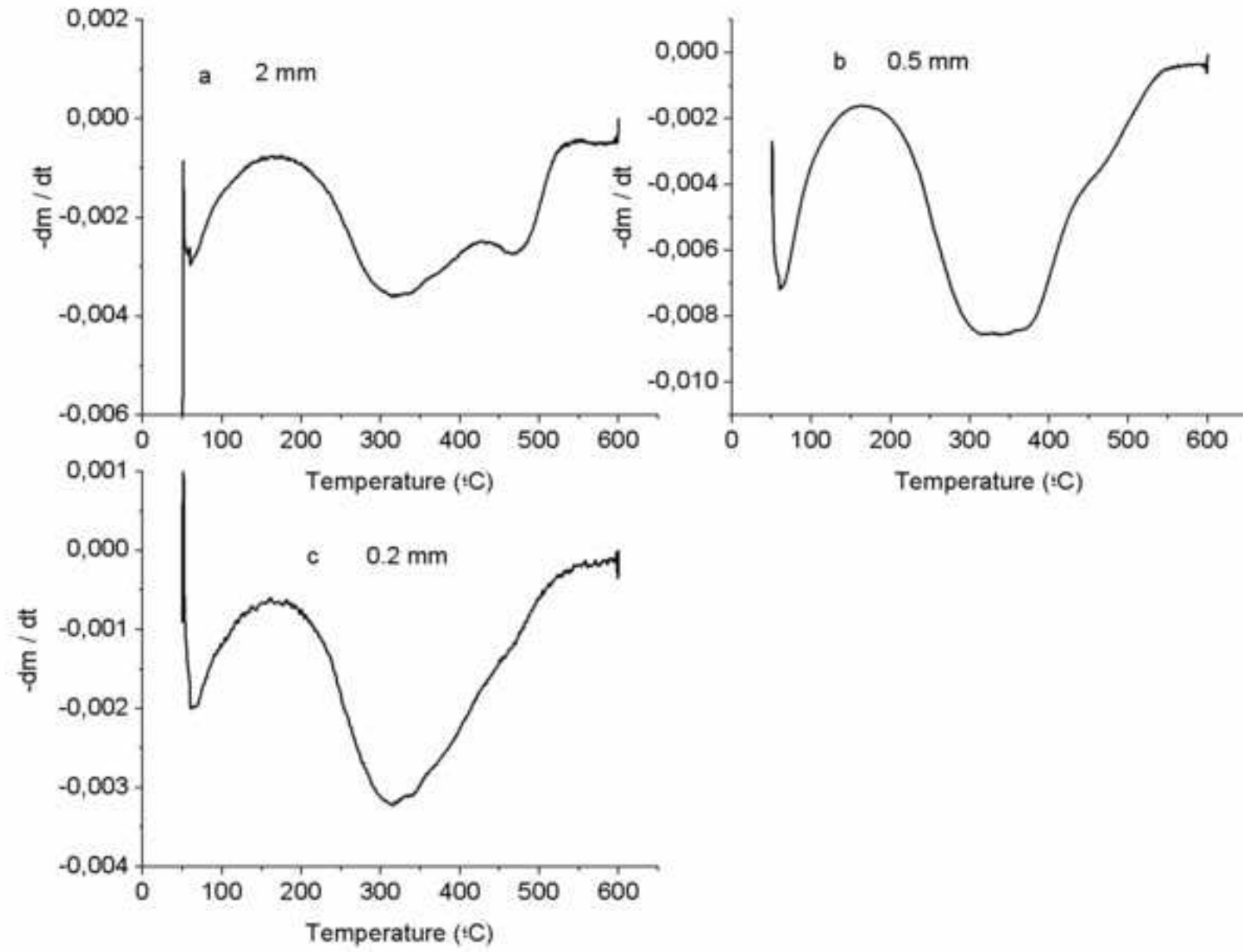


Figure

[Click here to download high resolution image](#)

Figure

[Click here to download high resolution image](#)



Figure

[Click here to download high resolution image](#)

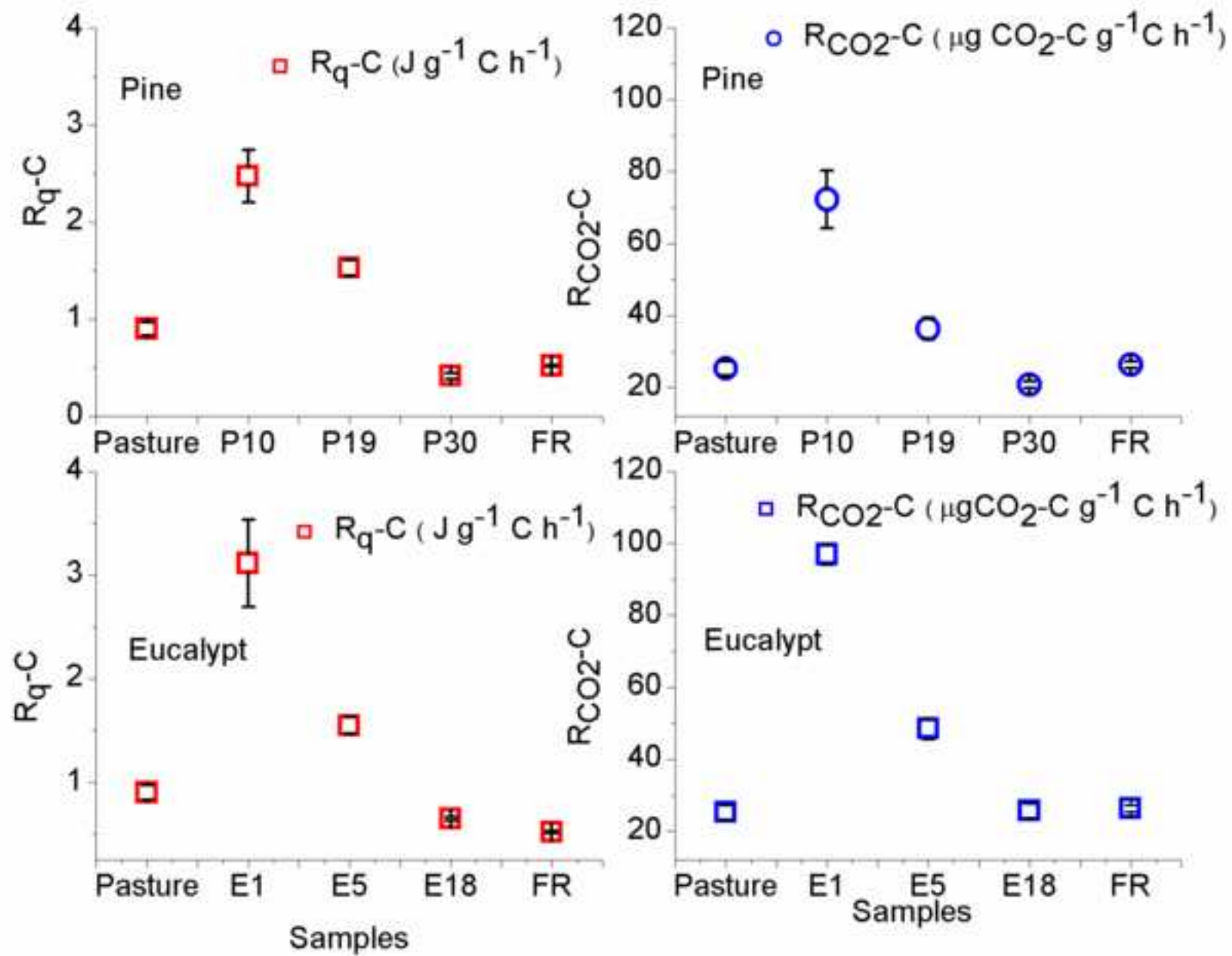


Figure
[Click here to download high resolution image](#)

